Available online at www.sciencedirect.com
ScienceDirect
Journal of Nuclear Materials 373 (2008) 112–118
journal of nuclear materials
www.elsevier.com/locate/jnucmat

Study of radiogenic helium diffusion in the β-thorium phosphate diphosphate ceramic

A. Özgümüs [a,*], E. Gilabert [b], N. Dacheux [a], C. Tamain [a], B. Lavielle [b]

[a] Université Paris-Sud 11, Institut de Physique Nucléaire, Groupe de Radiochimie, UMR 8608, Orsay F91405, France
[b] Laboratoire de Chimie Nucléaire Analytique et Bioenvironnementale, BP120 Le Haut Vigneau, Gradignan F33175, France

Received 27 February 2006; accepted 11 May 2007

Abstract

β-Thorium phosphate diphosphate polycrystalline ceramic is considered as a promising candidate for the immobilization of actinides in the field of a long-term storage. In order to study the behavior of the ceramic in relation with the evacuation of helium produced by actinides and daughters disintegrations, the release of radiogenic helium from a sintered pellet aged over an about six year period was studied by thermal desorption and high resolution mass spectrometry. The apparent diffusion coefficients are determined for different annealing sequences and are approximately the same for zircon and britholite at low temperature and uranium dioxide ceramic at high temperature. The apparent diffusion coefficients are found to be $(7 \pm 3) \times 10^{-22}$ m^2 s^{-1} and $(1.5 \pm 0.5) \times 10^{-20}$ m^2 s^{-1} at 20 °C and 120 °C, respectively. The activation energy for the apparent diffusion process encompassing both volume and inter-granular diffusion is estimated at 45 ± 15 kJ mol^{-1} in the studied temperature range (20–1020 °C).

PACS: 07.75; 23.60; 66.30

1. Introduction

Due to their very low propensity to dissolution in water, various thorium and uranium phosphates have been considered as potential candidates for the long-term storage of radionuclides such as actinides coming from the reprocessing of spent nuclear fuels. The expected temperature in the container is near 100 °C and the He concentration, for example, could reach 10^{19} atoms per gram for a Synroc ceramic containing 10 wt% of ^{239}Pu after a thousand years of storage [1]. Many of these compounds have been extensively studied in this context [2–9]. Among them, β-thorium phosphate diphosphate (β-TPD: β-$Th_4(PO_4)_4P_2O_7$), synthesized for the first time in our laboratory in 1994 [7], exhibits some main advantages: high resistance to aqueous alteration [10,11], thermal and chemical stabilities and good sintering properties (high density, low global porosity between 2% and 4%) [5]. The replacement of thorium by tetravalent actinides in the β-TPD structure leads to the formation of solid solutions of formulae $Th_{4-x}M_x(PO_4)_4P_2O_7$ (with M = U, Np or Pu). Up to 75, 52 and 41 mol% of replacement, for uranium, neptunium and plutonium, respectively, the solid remains as a single phase and most of the undoped β-TPD properties are conserved [12–14]. Small amounts of trivalent cations such as lanthanides and some actinides (Am, Cm) could be incorporated (less than 0.5 mol% [13]) without any modification of structure.

In all the cases, the large amount of radioactive elements generates a large quantity of helium by alpha-decay. The low solubility of this helium in most of the solids could form bubbles at high concentrations and could cause swelling and affect many of their physical properties. Spectacular examples are given by the external irradiation where the local concentration could form up to micrometrical bubbles (for a fluence of about 10^{22} He m^{-2} in AlSiON at 300 K [15] and 10^{20} He m^{-2} in Al_2O_3 at 900 K [16]). However, the accumulation of helium could modify first the

* Corresponding author. Tel.: +33 169 156504; fax: +33 169 157150.
E-mail address: ozgumus@in2p3.fr (A. Özgümüs).

0022-3115/$ - see front matter © 2007 Elsevier B.V. All rights reserved.
doi:10.1016/j.jnucmat.2007.05.038

nanostructure around point defects or dislocation loops by formation of clusters and microcavities [17]. Above all, for polycrystalline material (like β-TPD), these microcavities close to the grain boundaries could generate microcracks which finally modify the macroscopic structure and affect the mechanical properties of the ceramic. The present work deals with an un doped β-TPD ceramic aged over an about six year period in order to determine the diffusion coefficient and the activation energy for the apparent diffusion process of radiogenic helium. In this case, the radiogenic helium does not contribute to any structural effects due to the very low activity of the ceramic (less than 10^4 Bq g^{-1}).

2. Experimental

2.1. Synthesis and characteristics of the pellet

In our previous publications, we already reported several ways of synthesis of the β-TPD based on wet and dry chemical methods [7,8]. This compound can be synthesized after heating at high temperature (1250 °C) in air or under inert conditions, whatever the chemical way of synthesis, whatever the thorium salt used (thorium nitrate, chloride, bromide, oxalate, oxide, etc.) and the phosphating reactant (phosphoric acid, ammonium hydrogen phosphate, etc.) in the condition to respect the initial mole ratio $r = Th/PO_4$ equal to 2/3. The solid obtained after heating is always a well-crystallized, homogeneous and single phase. For all the other mole ratios, the system is polyphased. At this step, some divalent cations (like Ra, daughter of thorium – Fig. 2) could co-precipitate. Indeed, cations are trapped in the solid but are localized in the grain boundaries. Sintered sample was obtained from the residue prepared by the complete evaporation of the solution then heating treatment at 400 °C during 2 h. This precursor was first shaped into pellet form via a uniaxial room temperature pressing at 250 MPa. It was heated at 400 °C for 2 h, then up to 1250 °C for 10 h with a heating rate of 2–5 °C min^{-1}. The density and the specific surface area measurements were determined by using helium pycnometry and BET method with nitrogen adsorption, respectively. We determined either the effective or the apparent density to evaluate the open and closed porosities. The shape of the pellet is parallel epipedal and sized $4.3 \times 4.7 \times 13.6$ mm. The mean size of the grains is equal to 10 μm estimated from SEM microscopy and grain size distribution measurements. The open surface of the sample for He release is then equal to 0.084 m^2 and the mass of the pellet is equal to 1.40 g. The density of the pellet obtained reach 98% of the calculated value ($d_{calc} = 5.19$).

2.2. He measurements

He concentrations were measured using highly sensitive mass spectrometry. The noble gas facility includes essentially three parts: a sample heating, a gas cleaning device and a mass spectrometer all connected to a vacuum pumping system with turbomolecular and ionic pumps. All the parts of the system are made in stainless steel and are baked at 250 °C in order to reach very low residual pressure (from 10^{-12} bar in the heating zone to 10^{-13} bar in the mass spectrometer). For the gas release experiments from β-TPD, we used two stainless steel fingers heated by resistors at a maximum temperature of 1050 °C. After loading the samples, air is quickly pumped away and the experiment is done under static conditions using the following procedure. The extracted gases are cleaned successively with CuO, Pd and Ti powders at stepwise decreasing temperatures from 700 °C down to 350 °C and on Al–Zr getters working at 400 °C. This cleaning step is important to remove most of the residual gases such as O_2, N_2, CO_2 and H_2. Then, heavy noble gases (Ar, Kr, Xe) are trapped on charcoals at −196 °C and only a small fraction (to avoid the pollution of the cell) of the He released from the sample is introduced in the highly sensitive mass spectrometer for analysis. Then, the number of He atoms actually released is calculated after a very accurate volume calibration (uncertainty less than 1%). All the analyses are performed in a 12 cm radius and 60° magnetic sector Micromass 12 type mass spectrometer from Vacuum Generator equipped with an electron multiplier, and a microcomputer assisted peak switching. A typical analysis requires 60 min of heating time, 45 min for cleaning and 30 min for noble gas analyzing. The blank measurements were performed at different temperatures before introducing the sample and using the same extracting procedure. The number of atoms collected did not exceed 5×10^7–4×10^8. No correlation was found with temperature. Calibrations were made before and after analyses by measuring known quantities of air volume because of the precisely known constant quantity of rare gas in air. Uncertainties on the absolute concentration measurements are about 7% (including the volume calibrations and the statistical errors).

He measurements were performed on the same pellet. The results of several release experiments (series 1–4) involving a rapid increase in temperature followed by a hold period at that temperature are gathered in Table 1 and are plotted in Fig. 1. The room temperature experiments require long heating periods due to the very low diffusion process at 20 °C and the very low quantity of measured atoms induces a high uncertainty. The total quantity of He removed from the pellet during all the experiments is equal to $(1.6 \pm 0.1) \times 10^{12}$ atoms.

2.3. Thorium activity measurements

The He-generating radionuclides in the crystalline structure of β-TPD are mainly ^{232}Th and ^{228}Th from the ^{232}Th decay chain (Fig. 2), and ^{230}Th from the ^{238}U decay chain. In order to determine the quantity of He generated inside the pellet during ageing, the activities of these three isotopes at the pellet synthesis time (t_0) and at He

Table 1
Experimental details of He measurements, calculated apparent diffusion coefficients (D) for each temperature and activation energy (E_a) for each experimental series

Exp. series	Temperature (°C)	Heat duration (h)	He measured ($\times 10^8$ at/h)	Meas. uncert. (%)	D ($m^2\ s^{-1}$)	E_a (eV)
1	20	15.5	2.1	30	$(7 \pm 3) \times 10^{-22}$	0.47
	120	1	38	25	$(1.5 \pm 0.5) \times 10^{-20}$	
	320	1	900	7	$(8.5 \pm 2) \times 10^{-18}$	
2	20	12.5	0.24	150	$(1 \pm 2) \times 10^{-23}$	0.58
	520	1	2330	7	$(6.1 \pm 1) \times 10^{-17}$	
	720	1	2750	7	$(1.1 \pm 0.2) \times 10^{-16}$	
	910	1	3050	7	$(1.7 \pm 0.4) \times 10^{-16}$	
3	20	352	0.02	90	$(6 \pm 6) \times 10^{-24}$	0.55[a]
	1020	1	2080	7	$(1.2 \pm 0.3) \times 10^{-16}$	
4	520	68.5	10.2	7	$(2.8 \pm 0.6) \times 10^{-19}$	0.71
	820	22.5	105	7	$(1.1 \pm 0.3) \times 10^{-17}$	
	920	41.2	44	7	$(5.7 \pm 1) \times 10^{-18}$	
5	20	288	0.05	70	$(7 \pm 6) \times 10^{-23}$	

[a] Not enough values of D and too much difference between the two temperatures.

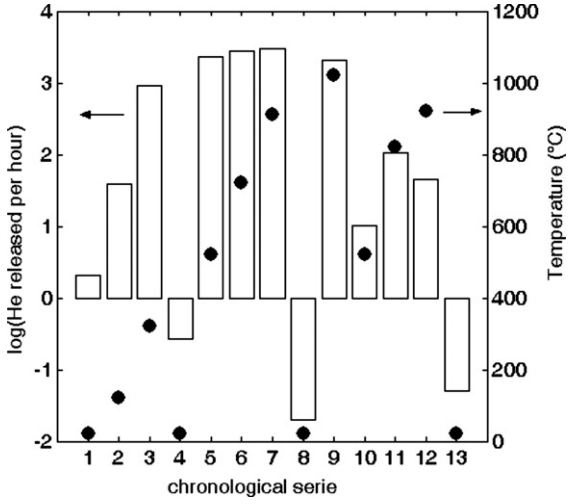

Fig. 1. He measurement results: bars represent the decimal logarithm of the quantity of He atoms measured per hour (left axes) and points represent the temperature of the heating step (right axis).

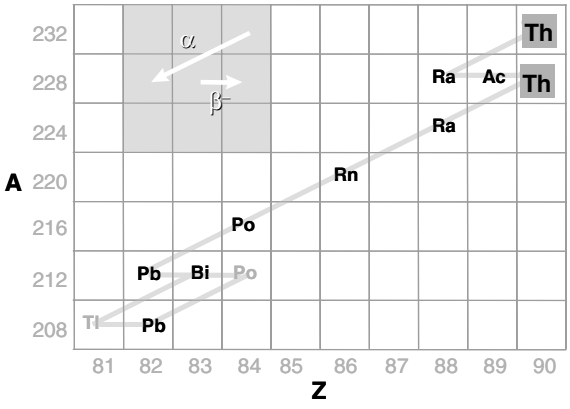

Fig. 2. Decay chain of thorium 232.

measurement time (t_m) must be determined. The mass of the sintered pellet is 1.40 g (62.6 wt% of Th) and the ^{232}Th concentration in the initial solution is equal to $(4.31 \pm 0.05) \times 10^{-1}$ mol L^{-1} (obtained by colorimetric method and alpha liquid scintillation). The activities of ^{230}Th (radioactive period, $T = 8 \times 10^4$ year) and ^{232}Th ($T = 1.39 \times 10^{10}$ year) were considered to be constant between t_0 and t_m, because of their long half-life. On the other hand, the activity of ^{228}Th must be precisely defined because of its own short half-life ($T = 1.91$ year) and the very short half-lives of all its five alpha emitting daughters (^{224}Ra – 3.6 d; ^{220}Rn – 55 s; ^{216}Po – 0.2 s; ^{212}Pb – 10.6 h; ^{212}Bi (33%) – 60 min and ^{212}Po (67%) – 0.3 μs). The measured and calculated values are reported in Table 2. PERALS® (Photon Electron Rejecting Alpha Liquid Scintillation) [18] and gamma spectrometry experiments were performed, respectively on the solution used for the synthesis of the

Table 2
Thorium isotopes and ^{228}Ra activities at t_0 and at t_m ($t_m - t_0 = 5.8$ year) in the pellet and in the solution

Element	Radioactive period (y)	Calculated activity at t_0 (Bq)	Measured activity at t_m (Bq)	Technique	From
^{232}Th	1.4×10^{10}	3570	3570 ± 290	α-Scintil./solution	4 MeV
^{230}Th	8×10^4	550	550 ± 45	α-Scintil./solution	4.7 MeV
^{228}Th	1.9	2850	3170 ± 260	γ-Spectr./solution	^{208}Tl (583 keV)
^{228}Ra	5.8	3100	3330 ± 270	γ-Spectr./solution	^{228}Ac (911 keV)
^{228}Th		2850	1450 ± 200	γ-Spectr./pellet	^{208}Tl (583 keV)
^{228}Ra		70	1950 ± 100	γ-Spectr./pellet	^{228}Ac (911 keV)

Activities were measured by γ-spectrometry or α-scintillation (PERALS).

ceramic (initial solution: $ThCl_4$) and on the pellet. PERALS technique discriminate easily 4 and 4.7 MeV α-particles with detection efficiency of about 100%. Gamma spectrometry measurements were performed in about 15 cm distance geometry calibrated system. Absorption of gamma rays in the sample is negligible due to the small size of the sample (1.4 g of solid and 100 μL of solution).

3. Diffusion coefficient

3.1. Theoretical background

The migration equation of noble gas in a given material comprises five components: intracrystalline diffusive transport (random molecular motion), advective transport (flow due to temperature gradient), convective transport (due to a pressure gradient), kinematic dispersion (depending on the heterogeneity of the microscopic velocities) and gas production term (for radiogenic gas). Due to the very low open porosity of the material (total porosity less than 4%, no cracks [6]), the advective and convective terms appear to be negligible. Due to the low thorium activities and to the very short He measurement experiment time, the production term can be also neglected. Finally, the homogeneity of the ceramic allows to neglect the kinematic term and to consider only the atomic diffusion process. Therefore, the Fick's second law under transient conditions governs the problem:

$$\frac{\partial C}{\partial t} = D\nabla^2 C, \tag{1}$$

where C is the concentration of He, D the diffusion coefficient, ∇^2 the Laplacian operator ($\nabla^2 \frac{\partial^2}{\partial x^2} + \frac{\partial^2}{\partial y^2} + \frac{\partial^2}{\partial z^2}$; x, y, z the spatial coordinates) and t is the diffusion time. For a semi-infinite solid, Eq. (1) could be reduced to a one-dimension problem [19]. Considering the initial and boundary conditions, the mathematical solution of this equation is [38]

$$\frac{C - Cs}{Co - Cs} = \mathrm{erf}\left(\frac{x}{2\sqrt{Dt}}\right), \tag{2}$$

- initial conditions: $t = 0,\ x > 0,\ C(x,0) = Co$
- boundary conditions: $\forall t > 0,\ x = 0,\ C(0,t) = Cs$

where erf is the error function (or Gaussian integral) defined as: $\mathrm{erf}(x) = \frac{2}{\sqrt{\pi}} \int_0^x \mathrm{e}^{-t^2}\,\mathrm{d}t$.

In our experimental conditions, helium is not accumulated at the surface of the solid ($Cs = 0$) and the He production term is neglected. The quantity of He escaped from the interface during a period t at a heat step i (Q_i) is given by the following equation:

$$\begin{aligned} &Cs = 0, \\ &Co_i = Co - Co_{(i-1)}, \\ &Q_i(t) = \int_0^t \frac{D_i Co_i}{\sqrt{\pi D_i t}}\,\mathrm{d}t = 2Co_i\sqrt{\frac{D_i t}{\pi}}. \end{aligned} \tag{3}$$

$Q_i(t)$ quantity of He released from the sample surface per unit area during annealing sequence i and diffusion period t (at m^{-2})

Co_i He-content in the matrix at step i recalculated after each heating sequence (at m^{-3})

D_i diffusion coefficient for the temperature corresponding to annealing step i ($m^2\ s^{-1}$)

t diffusion time or duration of the heating step i (s)

The diffusion coefficient D_i for each temperature could be calculated from the computed value of Co_i (Table 1). The calculation of the Co value is detailed in the following section.

3.2. Calculated He-content in the pellet

To determine with a good accuracy the He-content in the ceramic just before diffusion experiments (at t_m), the activity of the He-emitting nuclei at the time t_0 when the pellet was manufactured must be known and integrated over the period $t_m - t_0$. Bateman's equation [20] is applied to the solution. This enables the determination of the concentrations of all the relevant daughter nuclei of ^{232}Th, i.e., ^{228}Ra and ^{228}Th. By expressing the fact that the activities of ^{228}Ra, $A_{Ra\text{-}228}$, and ^{232}Th, $A_{Th\text{-}232}$, are known at t_m (Table 2), t_m can be computed Eq. (4):

$$A_{Ra\text{-}228}(t_m) = A_{Th\text{-}232}\left(1 - \mathrm{e}^{\lambda_{Ra} t_m}\right). \tag{4}$$

The knowledge of the activities of ^{228}Ra and ^{228}Th at t_m enables the determination of the ^{228}Ra and ^{228}Th activities in the pellet (Fig. 3). t_0 could be obtained by expressing the fact that the activities of ^{228}Th are equal in the solution and the pellet at $t = t_0$ and also ^{228}Ra activity in the pellet is equal to zero at t_0. However, due to the co-precipitation of Ra (calculated value 2%), the experimental results mismatch with the latter theoretical calculation of t_0. We know precisely the age of the pellet (5.8 year). Eq. (4) yields with $t_m = 22.4$ year. Thus, at t_0 (22.4 − 5.8 = 16.6 year), one can

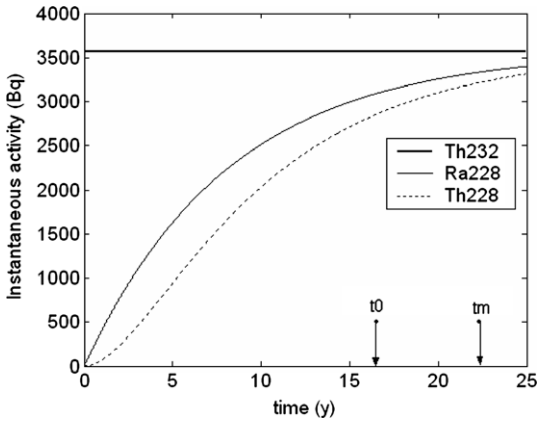

Fig. 3. Theoretical activities of ^{232}Th, ^{228}Ra and ^{228}Th in the solution since the equilibrium breaking (calculated) between ^{232}Th and ^{228}Ra. The synthesis time ($t_0 = 16.5$ year) and the He measurement time ($t_m = 22.3$ year) are indicated.

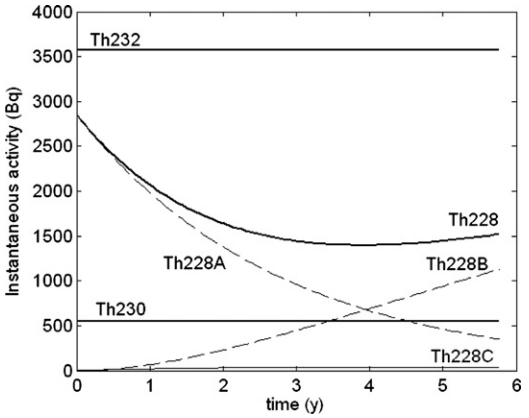

Fig. 4. Theoretical activities of ^{232}Th, ^{230}Th and ^{228}Th in the pellet ($t_0 = 0$, $t_m = 5.8$ year). Th228 is the sum of Th228A, Th228B and Th228C which represent initial ^{228}Th, ^{228}Th from decay of ^{232}Th and ^{228}Th from decay of initial ^{228}Ra, respectively.

calculate also with Eq. (4), the activities of ^{228}Ra and ^{228}Th in the solution to be equal to 3100 Bq and 2850 Bq, respectively (values reported in Table 2). Finally, at $t = t_0$, the calculated activities of Th isotopes in the pellet are equal to 3570, 550 and 2850 Bq, respectively for ^{232}Th, ^{230}Th and ^{228}Th and 70 Bq for ^{228}Ra (Table 2). The evolution of the instantaneous activity of Th isotopes is presented in Fig. 4. 'Th228' refers to the sum of 'Th228A' (Th-228 initially present at t_0), 'Th228B' (^{228}Th produced by decay of ^{232}Th) and 'Th228C' (^{228}Th produced by decay of initially co-precipitated ^{228}Ra). The cumulated He atoms in the pellet can be calculated by integrating these activities over the time (Fig. 5 and Table 3). Indeed, the major He-generator elements during this period of about 6 year is the ^{228}Th due to its short half-life and its daughters (^{224}Ra, ^{220}Rn, ^{216}Po, ^{212}Bi and ^{212}Po) and also ^{232}Th due to its high concentration. The contribution of ^{230}Th appears to be minor due to its low concentration and to long daughter half-life ^{226}Ra ($T = 1620$ year).

Table 3
Cumulative number of disintegrations N_i and quantity of generated He (N_α) in β-TPD

Element	N_i ($\times 10^{11}$)	N_α ($\times 10^{11}$)
^{228}Th	3.1 (×5)	15.5
^{230}Th	1.0 (×1)	1.0
^{232}Th	6.5 (×1)	6.5
Total		$(2.3 \pm 0.2^{a}) \times 10^{12}$ at

[a] Due to Δ[Th] in the solution, Th extraction process and α-scintillation measurement statistics [18].

4. Results and discussion

The apparent diffusion coefficients are calculated according to Eq. (3) where $C_0 = 2.3 \times 10^{12}$ atoms (Co_i is calculated after each heat step). These values are approximately the same as in zircon and in britholite samples at low temperature [22,34] and sintered uranium dioxide at high temperature [21]. The main uncertainties on the D value result from the propagation of relative uncertainties on the concentration of He in the pellet (about 8%) and on the He measurement experiments (Table 1). An Arrhenius-type plot for the diffusion coefficients in the temperature range studied (20–1020 °C) leads to an activation energy of (45 ± 15) kJ mol^{-1} (0.47 eV). This value is comparable to that determined in glasses. The significant uncertainty is due to the wide dispersion of the D values over all the series (Fig. 6). It is clear that the mean activation energy does not concern an unique diffusion phenomenon. But, the calculation of the activation energy separately for each series reduces by more than a factor 2 the uncertainty and gives 45, 56, 53 and 68 kJ mol^{-1}, respectively for series 1, 2, 3 and 4 (Table 1). This is the reason why an interval is given in Table 4 for this data. The calculated low activation energy is comparable to that in glass probably due to the abundance of grain boundaries of this polycrystalline ceramic of about 10 μm grains size. The temperature dependence of the calculated apparent diffusion coefficient is as

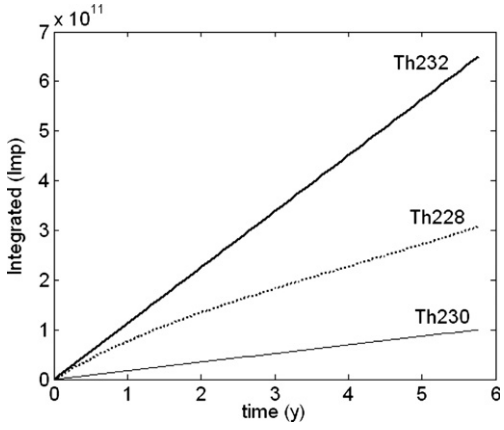

Fig. 5. Calculated number of disintegrations for ^{232}Th, ^{230}Th and ^{228}Th in the pellet between t_0 and t_m (integration of the curves in Fig. 3 over the time in second).

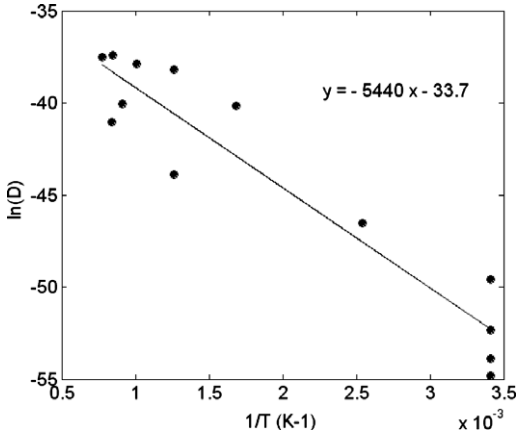

Fig. 6. Arrhenius-type plot for the diffusion coefficients in the studied temperature range (20–1020 °C). The activation energy of the diffusion of He in the β-TPD pellet is equal to 45 ± 15 kJ mol^{-1}.

Table 4
Activation energy and diffusion coefficient of He in several materials

Material	Temperature (°C)	D ($m^2 s^{-1}$)	Activation energy (eV)	Radiogenic: R Implanted: I	Reference
β-TPD	20	7×10^{-22}	0.5–0.7	R	This work
β-TPD	1020	10^{-16}		R	This work
UO_2	1000	3×10^{-17}	2	I	[21]
Britholite	200	10^{-19}	1.1	I	[22]
WC, W	20	10^{-17}	0.7	I	[23]
$MgAl_2O_4$	1000		2	I	[24]
V (crystal)	700	5×10^{-7}	0.2	I	[25]
Titanite	200		1.9	R	[26]
Apatite	300		1.6	R	[27]
Diamond	1300	3×10^{-21}	4.4	I	[28]
Olivine	1200		5.2	Trapped	[29]
Ni (polycrystal)	1000		0.8	I	[30]
Basaltic glass	200		0.6		[31]
Vitreous B_2O_3	20		0.8	Permeation	[32]
Tektite glass	20	4×10^{-14}	0.3	R	[33]
Zircon	105	3×10^{-22}		R	[34]

expected (increase with increasing temperature) except for the fourth series indicating a decrease by more than one order of magnitude. This temperature dependence does not exhibit several regimes as we can find in several materials externally irradiated with He-ions at high doses (irradiation damages bring to He transport other thermal dependent processes like defect production or defect annealing [21–25]). Thus, the limited solubility of He in many ceramics (0.5 at.%) and irradiation damages lead to a microscopic and macroscopic swelling that may result in cracking of the material [35–37]. These phenomena could change the diffusion processes: a second term related to the defects appears in the transport equation. The problem becomes more complicated because apparent diffusion coefficient and activation energy could not be ascribed to a given transport phenomenon (only atomic diffusion as considered in this work) in a given media (crystalline lattice and grain boundaries in this work).

More close to our subject, Roudil et al. [21] observed a decrease of the He diffusion coefficient with increasing the dose of irradiation (low dose, defect-free He-irradiation). After these authors, this is due to the clustering effect of He and the trapping around the created point defects. This clustering effect, enhanced by the high mobility of atoms at high temperature and for a long heating time at high temperature, could explain the significant decrease of the diffusion coefficients obtained for the last series of our results. Indeed, we observed significant changes of calculated D value after series 3 (Table 1) probably due to the long heating duration in the beginning of the series 4 (several tens of hours). Activated energy, calculated after D, exhibits also the same trend. Another explanation could be also the grain size dependent diffusion. The disorganized area represented by the grain boundaries where the gas could easily diffuse is inversely proportional to the grain size as highlighted by experiments on uranium dioxide [26]. In our experiments, the long heating time at high temperature for the fourth series could induce an increase of the grain size of the ceramic as shown by previous experiments on powdered β-TPD, where the average grain size increases by a factor of three when the temperature increases from 900 °C (5 μm) to 1250 °C (16 μm) for heating period of 10 h [5]. This hypothesis should be verified on the ceramic in a future work.

To simulate the storage condition, the potential effects of radiation for an actinide loaded pellet must be considered. On this subject, additional experiments with an external He-ion (also Kr-ion) irradiated and β-TPD pellets, doped with large plutonium contents are now in progress.

5. Conclusion

The radiogenic helium release of undoped thorium phosphate diphosphate sintered pellet aged over an about 6 year period was measured with a highly sensitive mass spectrometry technique in order to calculate the diffusion coefficient of He and to obtain the activation energy associated to the diffusion process. This is a preliminary study of the behavior of this material during the build-up of this gas as it would occur during the use as a long-term actinide storage matrix. The atomic diffusion coefficients are determined by applying Fick's second law and the continuity equation. In our case, He could not form bubbles due to its limited concentration (2×10^{12} atoms) and is homogeneously distributed inside the matrix (radiogenic He). Moreover, the matrix contains any defects (low porosity and no macroscopic irradiation damage). Thus, the He release from β-TPD pellet leads to the following apparent diffusion coefficients: $(7 \pm 3) \times 10^{-22}$ $m^2 s^{-1}$ at 20 °C and $(1.5 \pm 0.5) \times 10^{-20}$ $m^2 s^{-1}$ at 120 °C while the activation energy for the combined volume and inter-granular diffusion is (45 ± 15) kJ mol^{-1}. Radiogenic He diffusion coefficients are seldom reported in the literature and are usually difficult to compare (Table 4). Nevertheless, the values obtained during this work are almost the same as in zircon and in britholite at low temperature [22,34] or

sintered uranium dioxide at high temperature [21]. The calculated low activation energy is comparable to that in glass.

References

[1] W.J. Weber, R.C. Ewing, C.R.A. Catlow, T. Diaz De La Rubia, L.W. Hobbs, C. Kinoshita, Hj. Matzke, A.T. Motta, M. Nastasi, E.H.K. Salje, E.R. Vance, S.J. Zinkle, J. Mater. Res. 13 (1998) 1434.

[2] R.C. Ewing, W.J. Weber, F.W. Clinard, Progr. Nucl. Energy 29 (1995) 63.

[3] A. Meldrum, A. Boatner, J. Weber, R.C. Ewing, Geochim. Cosmochim. Acta 62 (1998) 2509.

[4] J.-M. Montel, J.-L. Devidal, D. Avignant, Chem. Geol. 191 (2002) 89.

[5] N. Dacheux, B. Chassigneux, V. Brandel, P. Le Coustumer, M. Genet, G. Cizeron, Chem. Mater. 14 (2002) 2953.

[6] N. Clavier, N. Dacheux, P. Martinez, E. Du Fou de Kerdaniel, R. Podor, Chem. Mater. 16 (2004) 3357.

[7] P. Bénard, V. Brandel, N. Dacheux, S. Jaulmes, S. Launay, C. Lindecker, M. Genet, D. Louër, M. Quarton, Chem. Mater. 8 (1996) 181.

[8] V. Brandel, N. Dacheux, M. Genet, E. Pichot, J. Emery, J.-I. Buzaré, R. Podor, Chem. Mater. 10 (1998) 345.

[9] V. Brandel, N. Dacheux, M. Genet, R. Podor, J. Solid State Chem. 159 (2001) 139.

[10] A.C. Thomas, N. Dacheux, P. Le Coustumer, V. Brandel, M. Genet, J. Nucl. Mater. 281 (2000) 91.

[11] A.C. Thomas, N. Dacheux, P. Le Coustumer, V. Brandel, M. Genet, J. Nucl. Mater. 295 (2001) 249.

[12] N. Dacheux, V. Brandel, M. Genet, K. Bak, C. Berthier, New J. Chem. 20 (1996) 301.

[13] N. Dacheux, R. Podor, V. Brandel, M. Genet, J. Nucl. Mater. 252 (1998) 179.

[14] N. Dacheux, A.C. Thomas, V. Brandel, M. Genet, J. Nucl. Mater. 257 (1998) 108.

[15] P.B. Johnson, P.W. Gilberd, A. Markwitz, A. Raudsepp, I.W.M. Brown, Nucl. Instrum. and Meth. B 166&167 (2000) 121.

[16] N. Sasajima, T. Matsui, S. Furuno, K. Hojou, H. Otsu, Nucl. Instrum. and Meth. B 148 (1999) 745.

[17] A. van Veen, H. Schut, A.V. Fedorov, E.A.C. Neeft, R.J.M. Konings, B.J. Kooi, J.Th.M. de Hosson, Nucl. Instrum. and Meth. B 147 (1999) 216.

[18] N. Dacheux, J. Aupiais, Anal. Chem. 69 (1997) 2275.

[19] J. Philibert, Atom Movements – Diffusion and Mass Transport in Solids, Les Editions de Physique, 1991.

[20] H. Bateman, Proc. Cambridge Philos. Soc. 15 (1910) 423.

[21] D. Roudil, X. Deschanels, P. Trocellier, C. Jégou, S. Peuget, J.-M. Bart, J. Nucl. Mater. 325 (2004) 148.

[22] J.-M. Costantini, P. Trocellier, J. Haussy, J.-J. Grob, Nucl. Instrum. and Meth. B 195 (2002) 400.

[23] T. Ono, T. Kawamura, T. Kenmotsu, Y. Yamamura, J. Nucl. Mater. 290–293 (2001) 140.

[24] E.A.C. Neeft, R.P.C. Schram, A. van Veen, F. Labohm, A.V. Fedorov, Nucl. Instrum. and Meth. B 166&167 (2000) 238.

[25] V.M. Chernov, V.A. Romanov, A.O. Krutskikh, J. Nucl. Mater. 271&272 (1999) 274.

[26] P.W. Reiners, K.A. Farley, Geochim. Cosmochim. Acta 63 (1999) 3845.

[27] R.A. Wolf, K.A. Farley, D.M. Kass, Chem. Geol. 148 (1998) 105.

[28] S. Zashu, H. Hiyagon, Geochim. Cosmochim. Acta 59 (1995) 1321.

[29] S.R. Hart, Earth Planet. Sci. Lett. 70 (1984) 297.

[30] V. Philipps, K. Sonnenberg, J.M. Williams, J. Nucl. Mater. 107 (1982) 271.

[31] A. Jambon, J.S. Shelby, Earth Planet. Sci. Lett. 51 (1980) 206.

[32] J.E. Shelby, J. Non-Cryst. Solids 14 (1974) 288.

[33] J.H. Reynolds, Geochim. Cosmochim. Acta 20 (1960) 101.

[34] D.R. Humphreys, S.A. Austin, A.A. Snelling, J.R. Baumgardner, in: John Ivey Jr. (Ed.), Proceedings of the Fifth International Conference on Creationism, Pittsburgh, USA, 4–8 August 2003.

[35] R. Fromknecht, J.-P. Hiernaut, Hj. Matzke, T. Wiss, Nucl. Instrum. and Meth. B 166&167 (2000) 263.

[36] N. Sasajima, T. Matsui, S. Furuno, T. Shiratori, K. Hojou, Nucl. Instrum. and Meth. B 166&167 (2000) 250.

[37] E. Ishitsuka, H. Kawamura, T. Terai, S. Tanaka, J. Nucl. Mater. 283–287 (2000) 1401.

[38] R.E. Cunningham, R.J.J. Williams, Diffusion in Gases and Porous Media, Plenum Publ. Corp., 1980.